

Laminar-to-Turbulent Stability and Transition

Helen L. Reed

Professor

Aerospace Engineering
Texas A&M University

Support: AFOSR, AFRL, NASA Langley, NASA Dryden, Lockheed Martin
AFOSR/NASA National Center for Hypersonic Research in
Laminar-Turbulent Transition

TAMU Supercomputer Center

Pointwise, Aerosoft



Team

Professor William S. Saric

TAMU: Richard Rhodes, Tyler Neale, Andrew Carpenter, Matthew Roberts, Matthew Tufts, Aaron Tucker, Joseph Kuehl, Eduardo Perez, Dawn Peterangelo, Travis Kocian, Sai Patel

ASU: Greg Stuckert, Thomas Buter, David Fuciarelli, Timothy Haynes, Ian Lyttle, Hossein Haj-Hariri, Nay Lin, Ray-Sing Lin

Stanford: Bart Singer



Agenda

- Motivation
- Background
- Verification
- Validation
 - Receptivity
 - 2-D Flat Plate
 - 3-D Swept Wing
 - Flight Tests
- Summary



Motivation for Transition Work

Transition 1st Order Impact:

- Aerodynamic Drag and Control Authority
- Engine Performance and Operability
- Thermal Protection Requirements
- Structural Concepts and Weight

Example of Maneuvering RV:

- Heating and drag increase significantly at transition
~6X between peak turbulent and laminar heating rates
- Substructure failure due to excessive temperatures
if transition earlier than anticipated
- Added shielding mass



Motivation for Transition Work

Control:

Desire:

- Delay transition (LFC - fuel efficiency, long range)

- Encourage for enhanced mixing or separation delay

Most effective strategy:

- Capitalize on the physics

- Identify most unstable disturbances.

If laminar flow could be maintained on wings of transport aircraft, fuel savings of up to 25% would be obtained.

Transport aircraft drag

- 50% skin friction

- 40% of that from wings

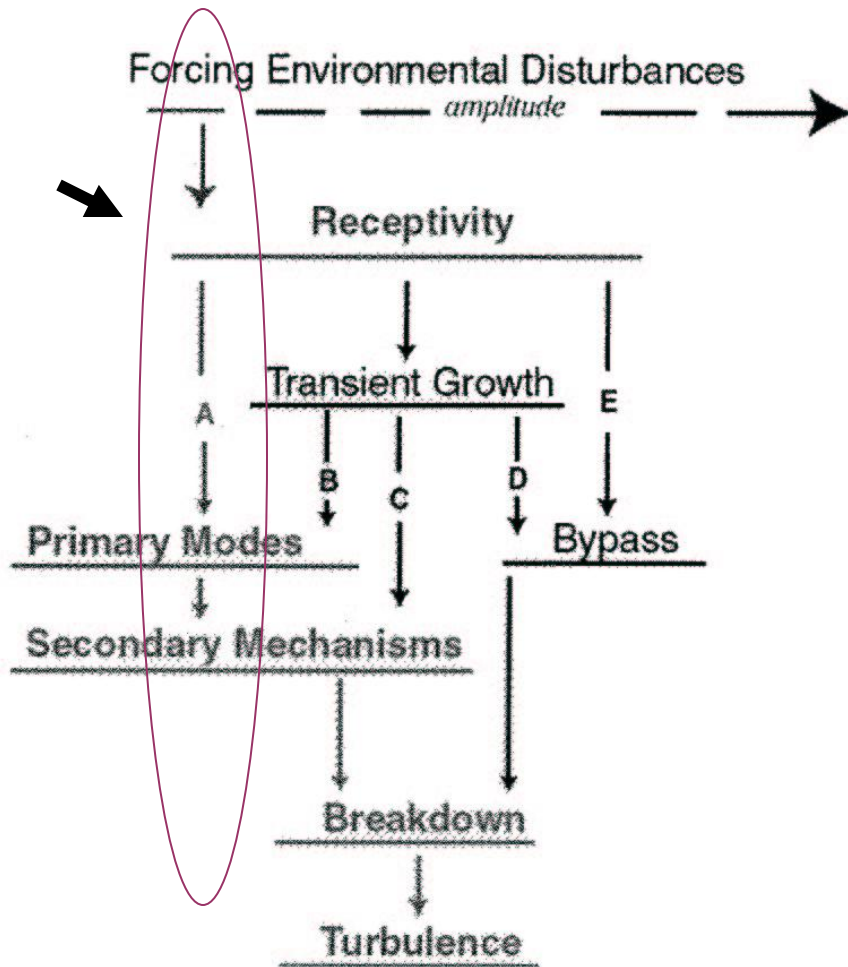


Motivation for Transition Work

- Of interest to turbulence community, boundary-layer flows are open systems, strongly influenced by freestream and wall conditions.
- Breakdown well documented to vary considerably when operating conditions change.
- Transition process then provides vital upstream conditions from which downstream turbulent flowfield evolves. Different transition patterns give rise to different turbulence characteristics.



Roadmap to Transition



- Receptivity - Disturbances in freestream (sound or vorticity) enter boundary layer as steady and/or unsteady fluctuations of basic state. Establish initial conditions of disturbance amplitude, frequency, phase.

flight, a few wind tunnels

$$u' < 10^{-3}$$

most wind tunnels $< 10^{-2}$

turbulent boundary layer $< 10^{-1}$

turbines/compressors $> 10^{-1}$

Roadmap to Transition

- Transition process highly dependent on operating conditions, wing and airfoil geometry, and surface conditions. Any prediction scheme must accurately account for relevant physics in each situation.
- Number of different instabilities can occur independently or together
- Facilities that minimize freestream disturbances to mimic flight must be used. Conventional tunnels can give trends opposite to flight.



Stability

- Basic State: Flow about which stability question is asked
 - Boundary layer, pipe flow, some solution of Navier-Stokes equations
 - Developed in-house or commercial
- Stability: Do small disturbances grow or decay in space or time?
- Procedure: Superpose small disturbances on basic state, solve



Verification

- Numerical accuracy of basic state must be very high, because stability and transition results very sensitive to small departures of mean flow from its “exact” shape.
- Stability of flow can depend on small variations of boundary conditions for the basic state, such as freestream velocity or wall temperature. Basic-state boundary conditions must also be very accurate.
- Example: For LFC, suction 10^{-3} to $10^{-4} U_{\infty}$
 - relative growth reduced from e^{26} to e^5 at $F = 10 \times 10^{-6}$



Verification

Basic State

- Commercial-code challenges
 - Documentation often limited
 - Usually run with only few points in boundary layer (too coarse)
- Recommend
 - Grid-refinement studies, different grid architectures
 - Change “far-field” boundary locations systematically and resolve
 - Solve test problems for which solution is known
 - Run unsteady code with time-independent boundary conditions
 - Run geometrically unsymmetric codes with symmetric conditions
 - Method of manufactured solutions (if in-house)
 - Test all appropriate options (if commercial)
 - ***Acid test: Do the stability results change?***

Stability Formulation (DNS, NPSE, ...)

- Be sure linear problem is correct



Validation

- Basis of validation is assumed to be successful comparison with careful, archival experiments
- Advances in basic mechanisms and prediction methods from working together, experiments and computations:
 - Transition highly sensitive to operating conditions. Computations provide validation of experiments and vice versa
 - Explanation of mechanisms easier to determine and simpler models thus developed, because each provides different level of detail and perspective
 - Very important to work on same geometries, and confirm it



Receptivity

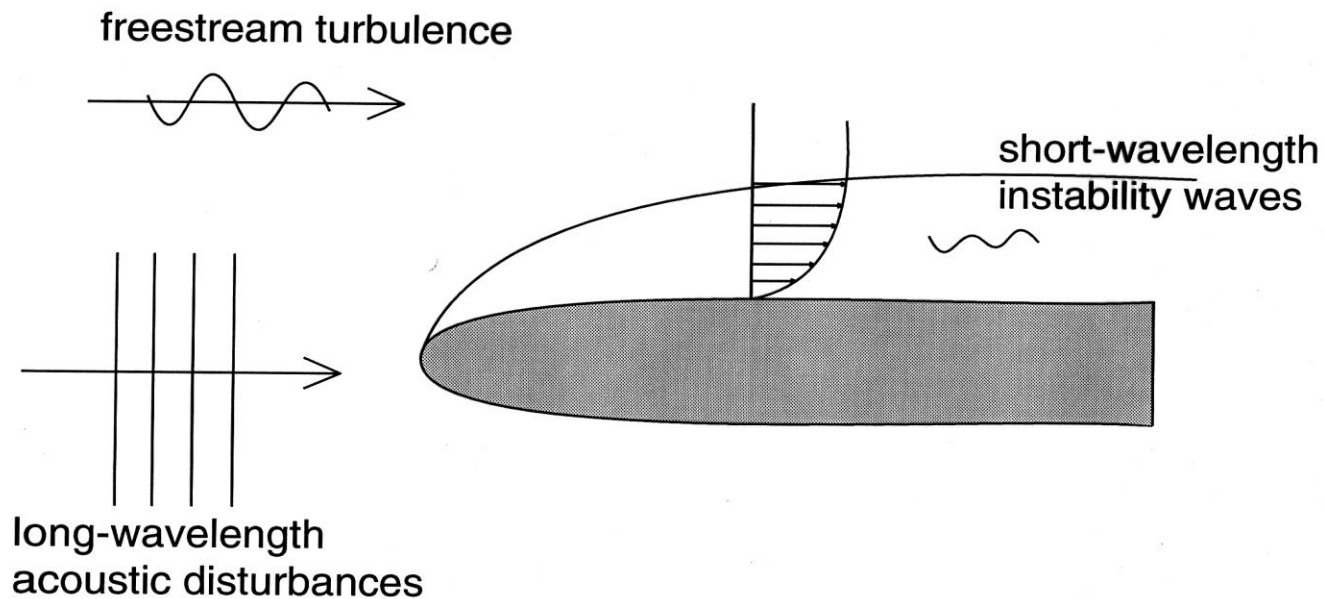
- Validation hampered by ability to connect freestream, surface conditions (e.g. roughness), and boundary-layer response
- Receptivity has many different paths through which to introduce disturbances into boundary layer. Among these, interaction of freestream sound or vorticity with
 - leading-edge curvature
 - discontinuities in surface curvature
 - surface inhomogeneities,
 -causes spectrum to broaden to include response wavenumber



Receptivity

Validation Example

Leading-Edge Receptivity to Sound



Receptivity

- Flat-plate LE receptivity to sound
 - Pioneering theory of Goldstein and Kerschen
 - Several unsuccessful DNS computational models
 - Assumed straight-line flat plate
 - Infinite vorticity at leading edge



Receptivity

- Flat-plate LE receptivity to sound
 - Spatial DNS means finite curvature can be included in LE region
 - Lin et al demonstrated that ellipse/LE juncture is receptivity source

AR = 6

Instantaneous Disturbance Streamlines
AR=6, F=230, after 4 cycles

CONTOUR LEVELS

-.03400
-.03200
-.03000
-.02800
-.02600
-.02400
-.02200
-.02000
-.01800
-.01600
-.01400
-.01200
-.01000
-.00800
-.00600
-.00400
-.00200
0.00000
0.00200
0.00400
0.00600
0.00800
0.01000
0.01200

0.000 MACH
0.00 DEG ALPHA
2.40x10**3 Re
170x70 GRID



AR = 6

Instantaneous Disturbance Streamlines
AR=6, F=230, continuous curvature

CONTOUR LEVELS

-.03400
-.03200
-.03000
-.02800
-.02600
-.02400
-.02200
-.02000
-.01800
-.01600
-.01400
-.01200
-.01000
-.00800
-.00600
-.00400
-.00200
0.00000
0.00200
0.00400
0.00600
0.00800
0.01000
0.01200

0.000 MACH
0.00 DEG ALPHA
2.40x10**3 Re
170x70 GRID

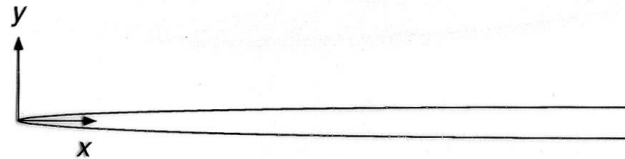


Flat-Plate Model

Leading-Edge Geometry

- The modified super ellipse (Lin et al, 1992)

$$\left(\frac{y}{b}\right)^2 + \left(\frac{a-x}{a}\right)^{2+\left(\frac{x}{a}\right)^2} = 1$$



- For 20:1: $a = 95.3$ mm, $b = 4.76$ mm
- For 40:1: $a = 190.5$ mm, $b = 4.76$ mm
- Isolate receptivity to the role of the leading edge
 - Eliminate leading-edge/flat-plate juncture discontinuity
 - Eliminate curvature discontinuity
 - Move pressure-recovery region closer to the leading edge

Receptivity

Flat-plate leading-edge experiments

- DNS will naturally assume symmetric flow around the leading edge (what else?)

SOLUTION: Have a trailing edge flap to control overall circulation and position of stagnation point

- measure differential pressure from two points on leading edge, one on test side, one on back side.
- check to see if it is independent of speed



Receptivity

Experiments

- Provide leading edge easy to model computationally
 - Schubauer & Skramstad and Klebanoff had drooped LE to avoid separation from sharp LE. Position of stagnation line unknown and hence x-location incorrect. Difficult to simulate computationally.
 - Ellipse with $AR > 6$ prevents leading-edge separation
 - Ellipse has zero slope at flat plate but non-zero curvature. Curvature discontinuity produces pressure spike and receptivity source (from computations). Experiments do polishing smoothing.

SOLUTION: Machine modified super ellipse with $AR > 6$ to front of flat plate. Select AR that both can model.



Receptivity

Experiments

– Receptivity Coefficient

- LE receptivity coefficient defined as ratio of T-S amplitude in LE region to freestream-sound amplitude
- Branch I receptivity coefficient defined as T-S amplitude at Branch I normalized with freestream-sound amplitude

Choose second one:

- It is impractical for experiment to measure first one
- Most transition correlation schemes begin with Branch I calculations
- Pressure-gradient history can be easily accounted for by linear stability theory calculations up to region near LE



Receptivity

Branch I receptivity coefficients for multiple frequencies as predicted by DNS and compared with experiments for 20:1 MSE

	Wanderley & Corke (2001)	Fuciarelli et al (2000)	Saric & White (1998)
Case	DNS	DNS	Experiment
F	90	82—86	88—92
K_i	0.046	0.048	0.050 ± 0.005

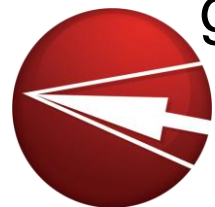


Complete integrated picture of geometry (including finite nose radius) and pressure gradients MUST be included

2-D Flat Plate

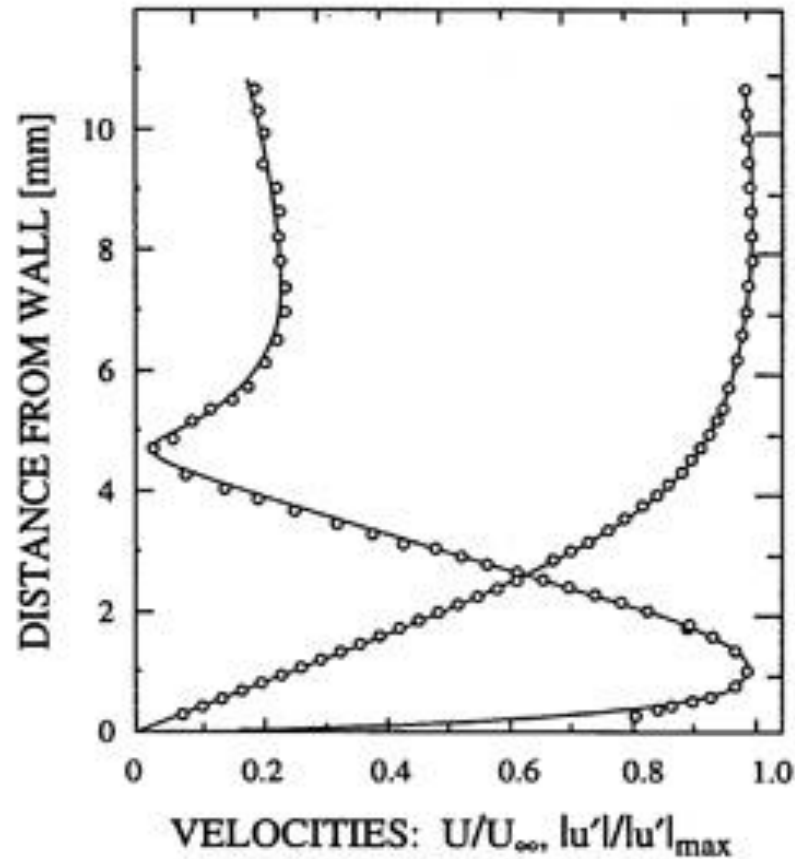
Experiments (Required reading: Saric “Wall-Bounded Flows: Boundary-Layer Stability and Transition”, Chapter 12.3, pp. 886-896, Handbook of Experimental Fluid Mechanics, eds. Tropea/Yarin/Foss, Springer, 2007)

- Whether objective is transition control, 3-D, secondary instabilities, nonlinear effects, or receptivity, two rules must always be followed:
 - Rule One
 - Get linear problem correct. Compare with theory. Sometimes weak pressure gradients or wind-tunnel wall discontinuities, undetected by basic state, affect stability. Correlation of *disturbance behavior* with linear theory will give indication that basic state is correct.



2-D Flat Plate

- Comparison of experiments with Blasius and LST



2-D Flat Plate

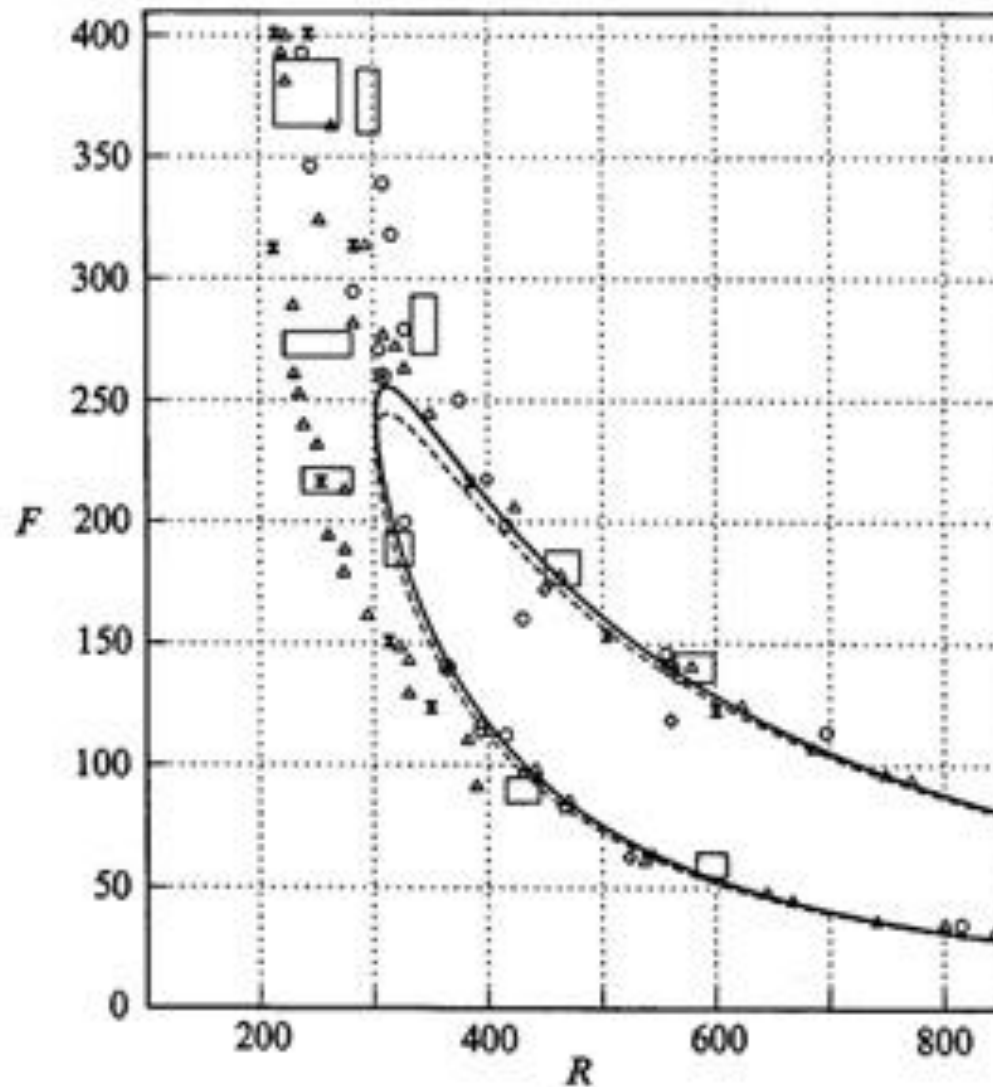
Experiments Saric (2007)

– Example

- Difficult to measure small changes in C_p
- 1% change in C_p over 100 mm corresponds to a Falkner-Skan pressure gradient parameter of +0.1
 - Min critical R changes by factor of 3, corresponding x changes by factor of 9.
- Saric suggests differences in experimental neutral curves due to local pressure gradient near LE
- **Solution:** Measure shape factor $H = \delta^*/\theta$.
 - F-S pressure gradient parameter = +0.1 corresponds to ΔH of 7%. Keep $H = 2.59$ ± 0.005



2-D Flat Plate



2-D Flat Plate

- Other effects
 - Use flat plate which is flat (manufacturing process)
 - Virtual leading edge
 - Leading-edge vibration
 - Turbulent wedges propagate from sidewall-LE junction and from disturbance source
 - Spanwise uniformity / symmetries
 - Hotwire-surface interactions
 - Sting/traverse blockage
 -



2-D Flat Plate

Experiments (Saric 2007)

- Rule Two
 - Full documentation of physical properties, background disturbances, initial amplitudes, and spatial variations must be provided to analyst
 - Need coordinate specifications i.e. wind-tunnel coordinates versus body-oriented coordinates.
 - Experimentalist should heed symmetry requirements often regularly assumed by analyst.
 - Includes spanwise periodic boundary conditions



2-D Flat Plate

Experiments (Saric 2007)

- Not until Schubauer & Skramstad constructed low-turbulence tunnel were T-S waves observed.
- Freestream disturbances are made up of irrotational (sound) and rotational (turbulence) disturbances. Measure each.
- Until we completely understand receptivity process, in addition to rms u one should quote, in order of importance:
 - passband and spectrum for all measurements (use lowest high-pass filter, 0.1 Hz; identify inertial sub-range)
 - spatial correlation to separate sound from turbulence
 - flat-plate transition Reynolds number
 - measurements of v and w



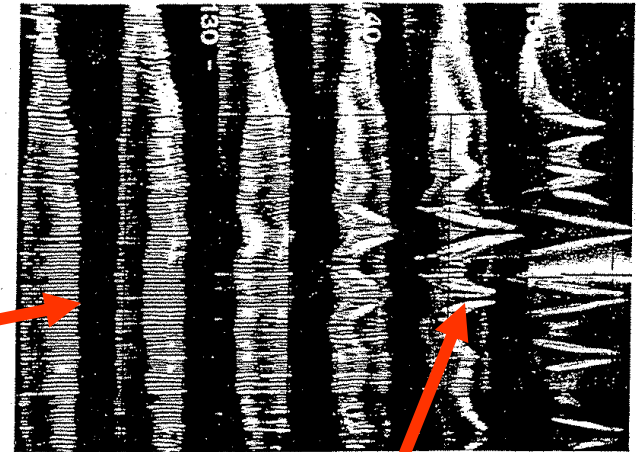
2-D Flat Plate

Irrotational parts of freestream disturbances (sound) contribute to initial amplitudes of 2-D T-S.

Vortical parts of freestream disturbances (turbulence) contribute to 3-D aspects of breakdown

Freestream sound and turbulence present different set of problems in predicting and controlling boundary transition and each require unusual experimental and computational techniques.

→
Flow



2-D Flat Plate

- Experiment predicts K-type
- DNS predicts H-type
- Singer et al. 1989 used combination of random noise and streamwise vortices as upstream conditions and showed that, depending on amplitude of vorticity, route to turbulence can be altered and experimental results matched.



Figure 10 (a)



Figure 10 (b)

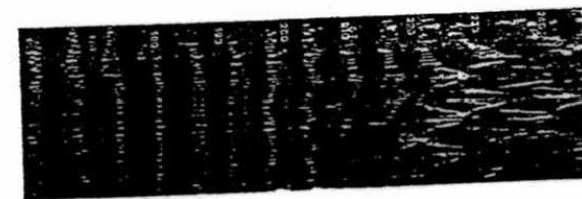


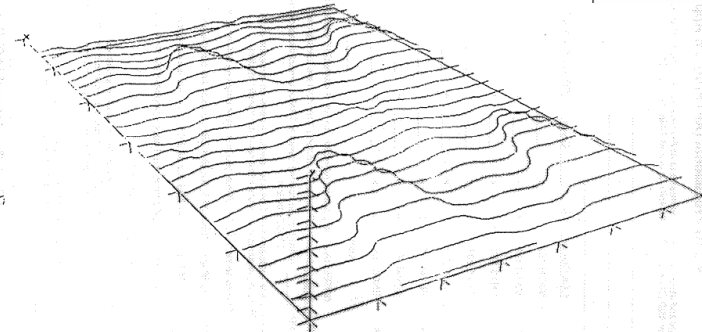
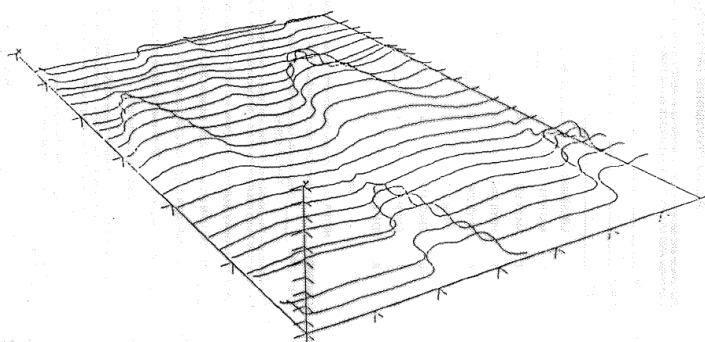
Figure 10 (c)



Figure (d)

1.00×10^{-3} Nu
 4.47×10^{-2} U_{tau}
 5.00×10^{-3} Re
 177.42 Time
 24x48x48 GRID
 A = 2%

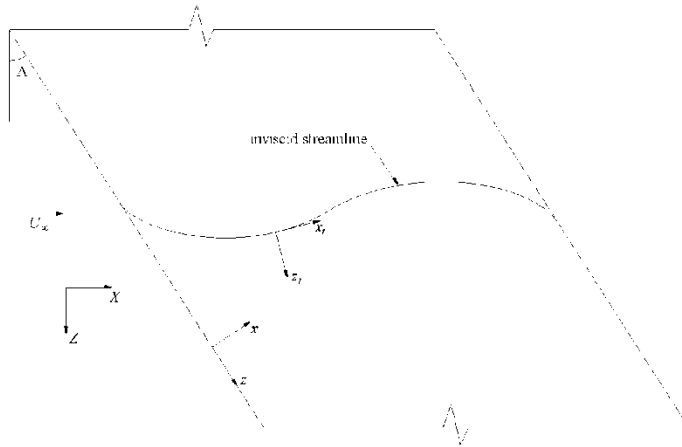
1.00
 4.47
 5.00
 132
 24x48



3-D Swept Wing

ASU Unsteady Wind Tunnel

Streamlines Over a Swept Wing



Leading-edge contamination

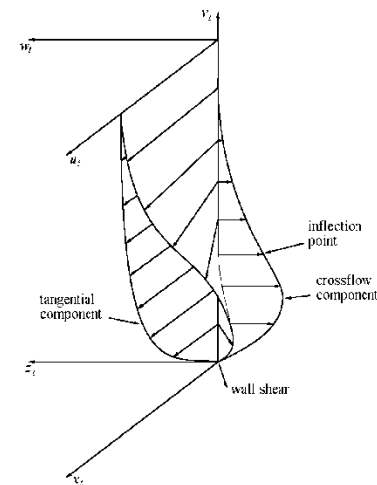
Streamwise instabilities

Crossflow instabilities

Curvature-induced instabilities

ASU Unsteady Wind Tunnel

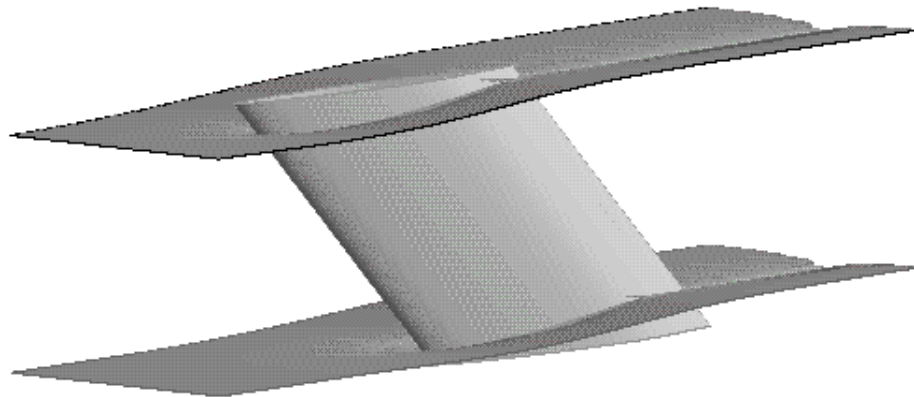
Swept-Wing Boundary Layer



3-D Swept Wing



- 45° sweep
- Favorable-pressure-gradient design produces strong crossflow, no other instabilities
- No taper, use root and tip wall liners
 - simulate infinite span for computational validation (periodic boundary conditions)

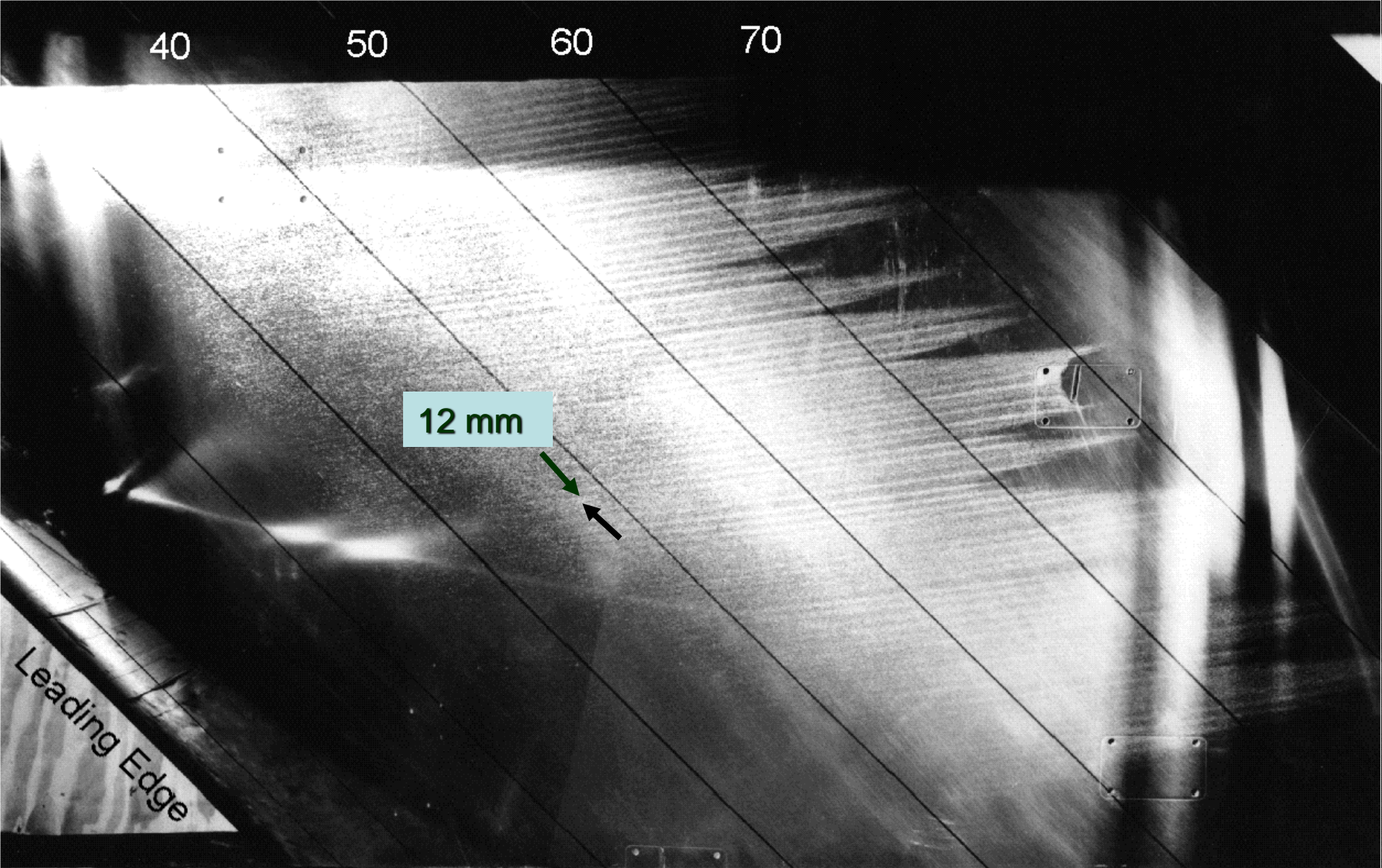


Klebanoff-Saric Quiet Wind Tunnel now at Texas A&M

3-D Swept Wing

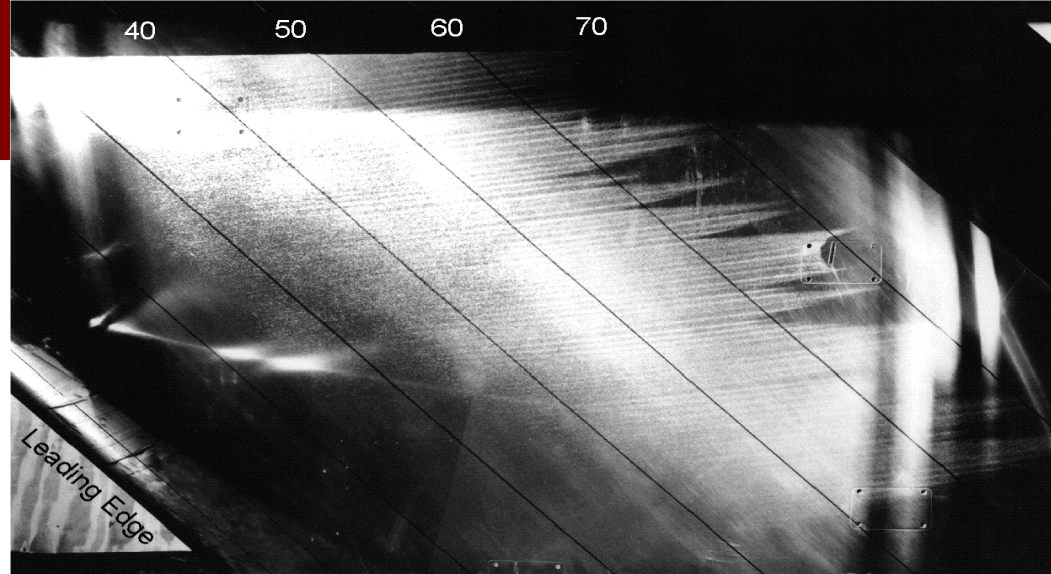
- Inviscid instability
- Linear stability theory
 - Traveling unstable waves predicted
 - Stationary ($\omega=0$) observed in flight
- Co-rotating vortices aligned with potential flow direction
 - Early development of nonlinear effects
- Sensitive to micron-sized roughness near LE. Insensitive to 2-D roughness. (Opposite to T-S)
- Sensitive to freestream vorticity. Insensitive to sound. (Opposite to T-S)





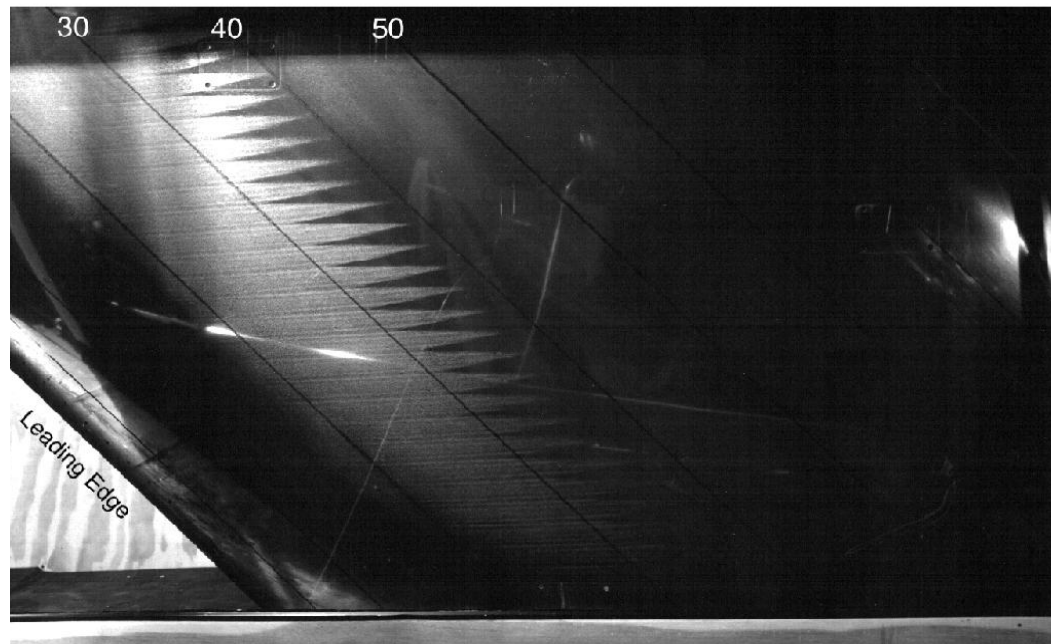
Naphthalene flow visualization for $Re_c = 2.4 \times 10^6$
and no artificial roughness.

No roughness



Periodic
boundary
conditions

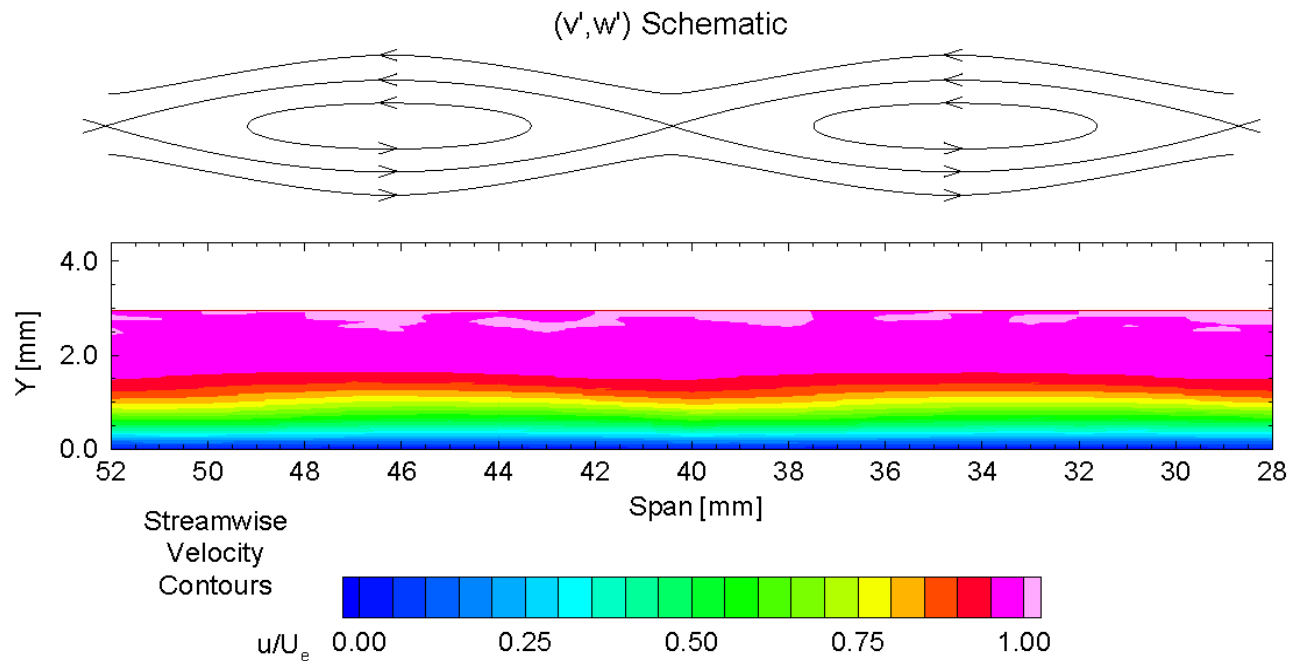
Roughness at
 $x/c = 0.023$,
36 mm spacing



Stationary Crossflow Waves

NLF(2)-0415 at $\alpha = -4^\circ$, $Re_c = 2.4 \times 10^6$, $x/c = 0.20$

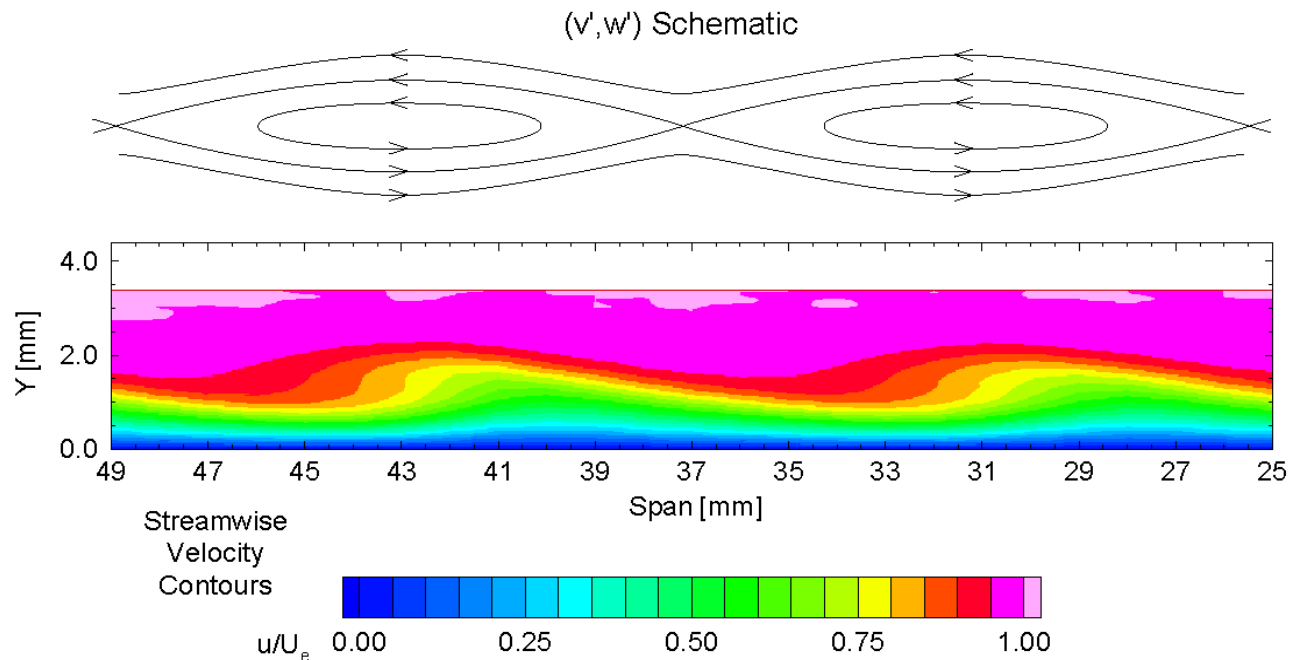
6 μm roughness at $x/c = 0.023$, 12 mm spacing



Stationary Crossflow Waves

NLF(2)-0415 at $\alpha = -4^\circ$, $Re_c = 2.4 \times 10^6$, $x/c = 0.30$

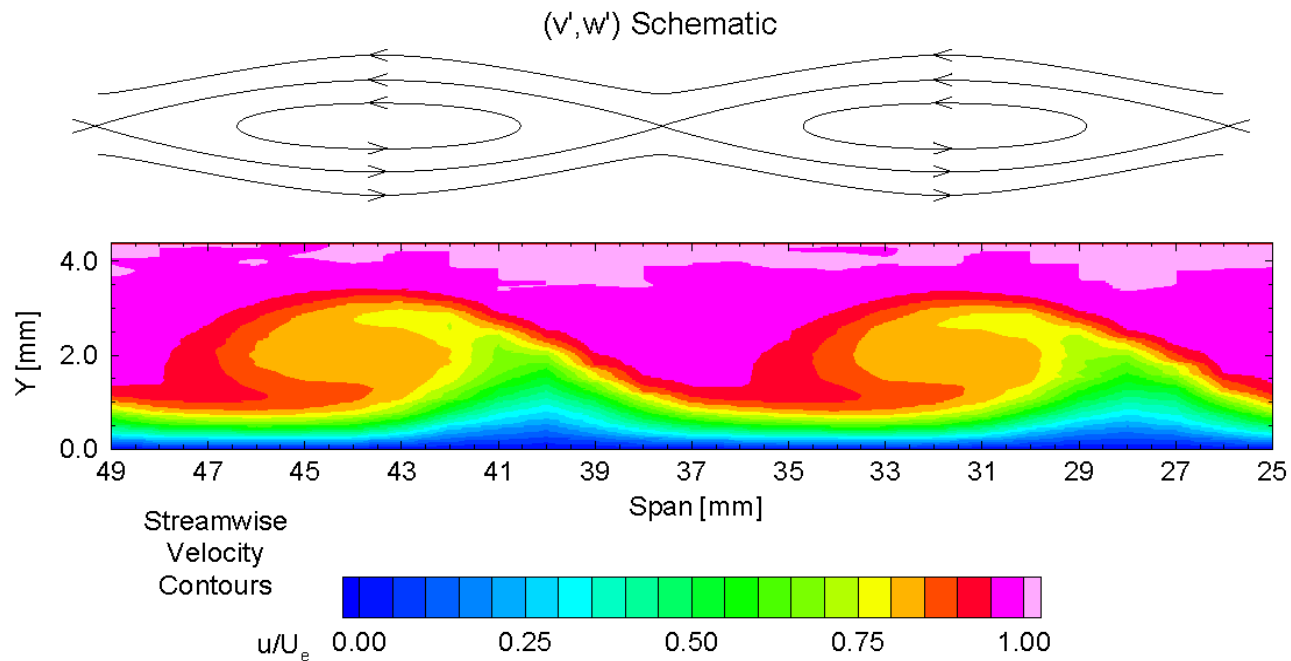
6 μm roughness at $x/c = 0.023$, 12 mm spacing



Stationary Crossflow Waves

NLF(2)-0415 at $\alpha = -4^\circ$, $Re_c = 2.4 \times 10^6$, $x/c = 0.45$

6 μm roughness at $x/c = 0.023$, 12 mm spacing

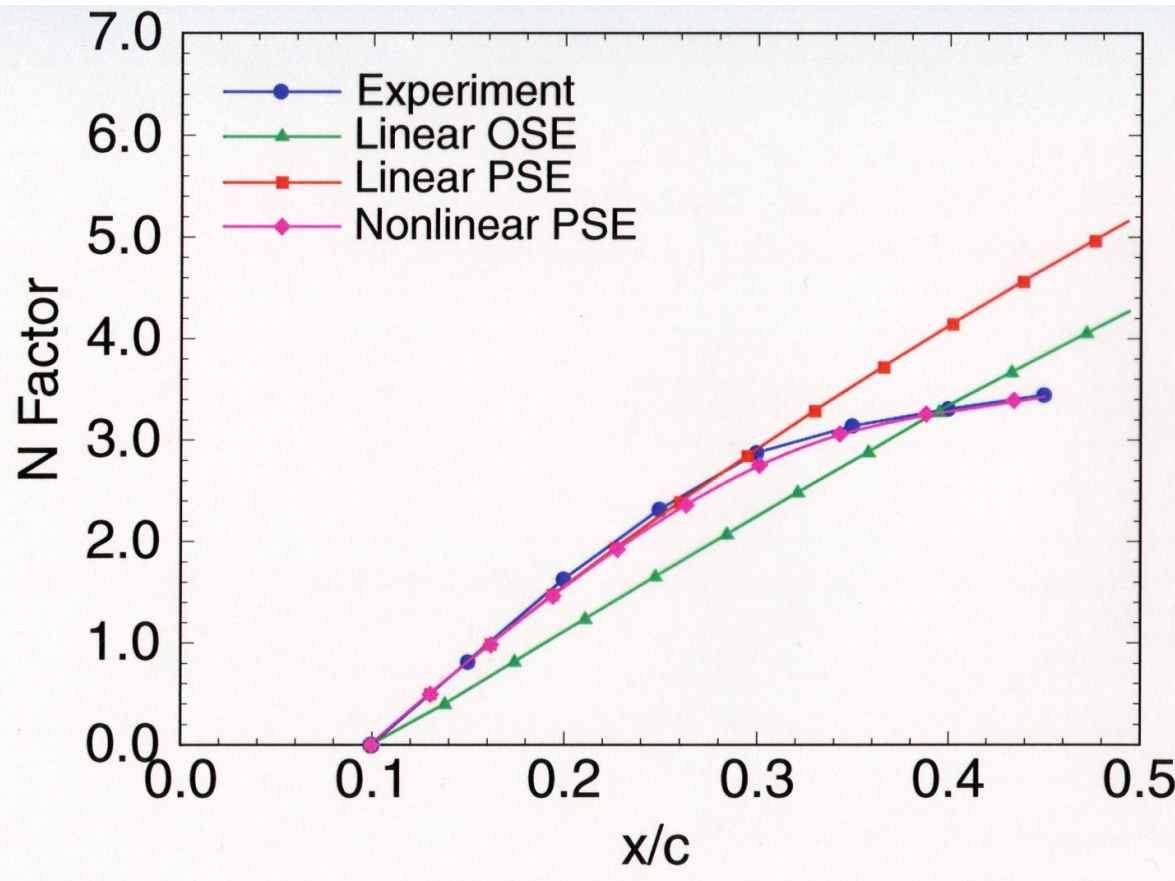


3-D Swept Wing

- Nonlinear Parabolized Stability Equations (NPSE)
 - Reduced set of Navier-Stokes equations
 - Low CPU and memory
 - Physics of boundary-layer behavior
 - high Reynolds numbers
 - nonlinear and nonparallel
 - effects of curvature
 - Obtain spatial and temporal scales



3-D Swept Wing



Effects:

- Lab coordinates vs body-fitted computational coordinates
- Model orientation
- Sidewall boundary layers: blockage

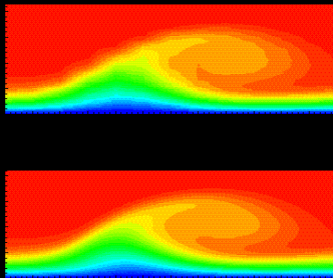
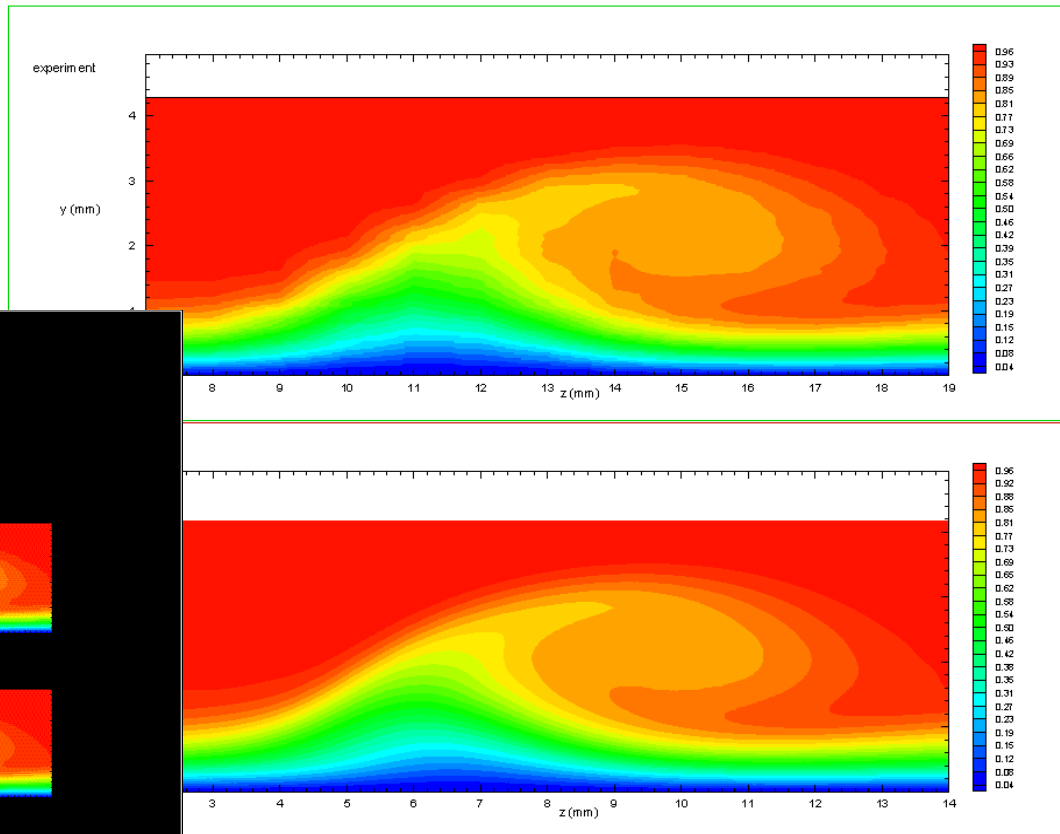


Total Streamwise Velocity Contours

NLF(2)-0415 at $\alpha = -4^\circ$, $Re_c = 2.4 \times 10^6$, $x/c = 0.40$

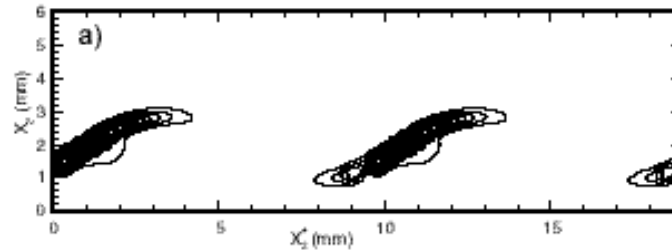
48 μm roughness at $x/c = 0.023$, 12 mm spacing

Computations include curvature

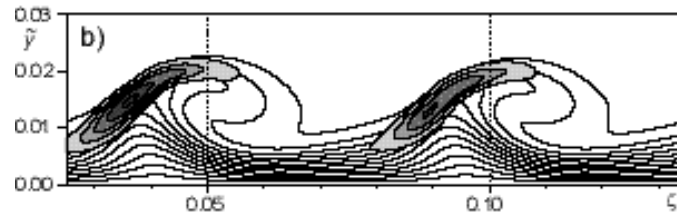


3-D Swept Wing

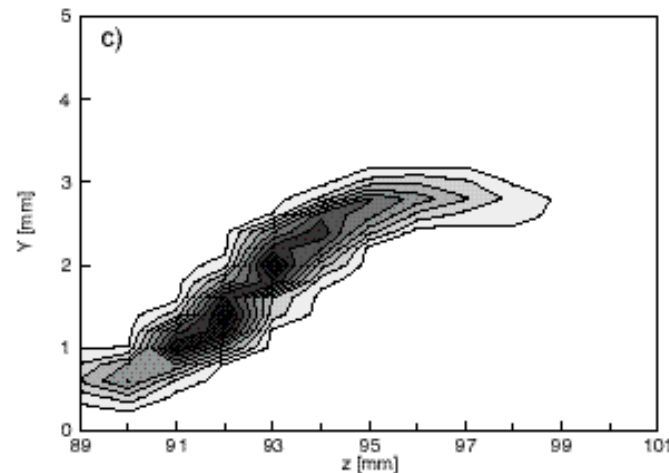
Malik et al (1999)



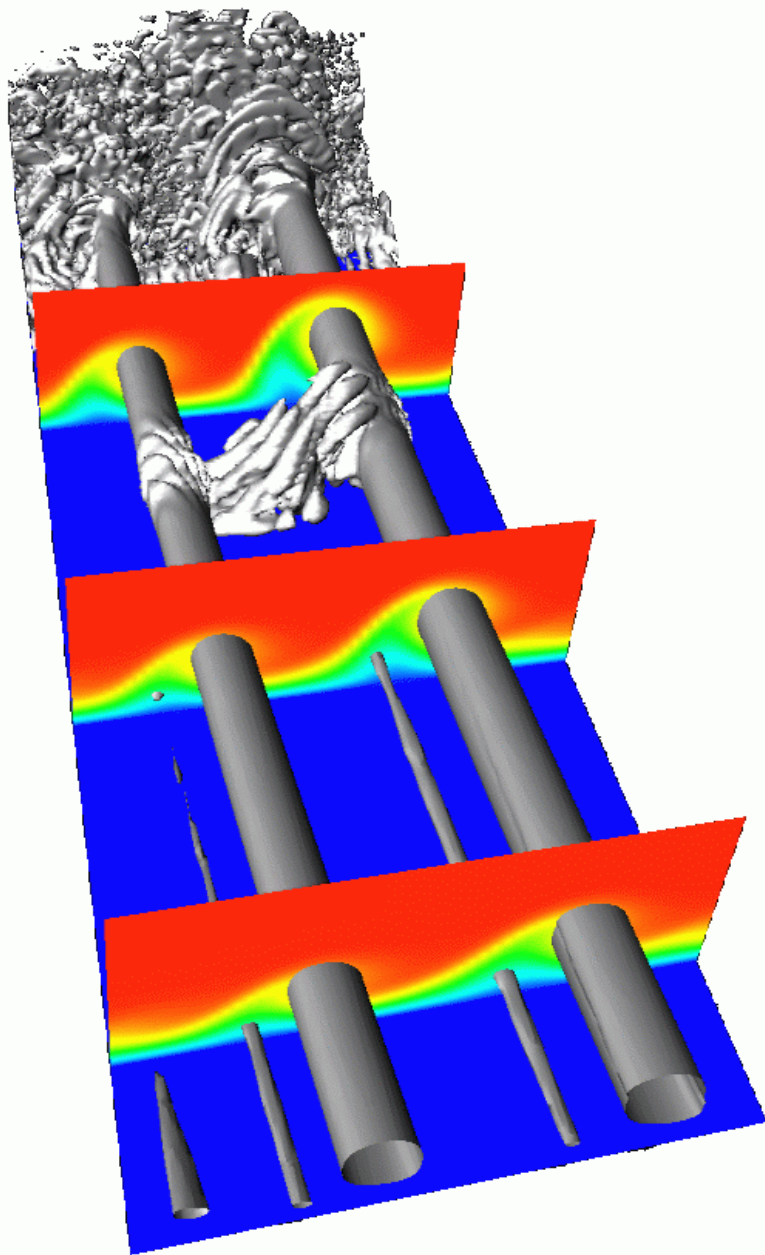
Wasserman & Kloker



Saric & White



Comparison shows agreement on location of breakdown and that associated with inflection point in spanwise direction (an extremum in $\partial U / \partial z$).



Various approaches to secondary instability problem (experimental, NPSE, DNS), have achieved rather remarkable agreement in basic mechanisms, unstable frequencies, mode shapes, growth rates.

Flight Tests

- Ongoing program
 - Do higher Re crossflow experiments at turbulence levels lower than wind tunnels
 - Even best tunnels challenged when $M > 0.25$
 - Establish flight research capability
 - Atmospheric turbulence essentially large scale
 - Turbulence scales that effect boundary layer are missing



Flight Tests



- Team-member for LFC flights tests of
 - NASA Dryden F-15B flight test M 1.6
 - Swept-wing model mounted below port wing of Cessna O-2 aircraft at Texas A&M's Flight Research Laboratory
 - Re_c up to 7.5 million: High-altitude, long-endurance UAVs
 - Swept glove mounted to port wing on NASA G-III
 - Re_c 22-30 million: Business jets
 - Model design and computations of physics based on DNS (basic state), LST, NPSE
 - Recommend: Instrumentation kinds and placement, manufacturing tolerances, operating ranges



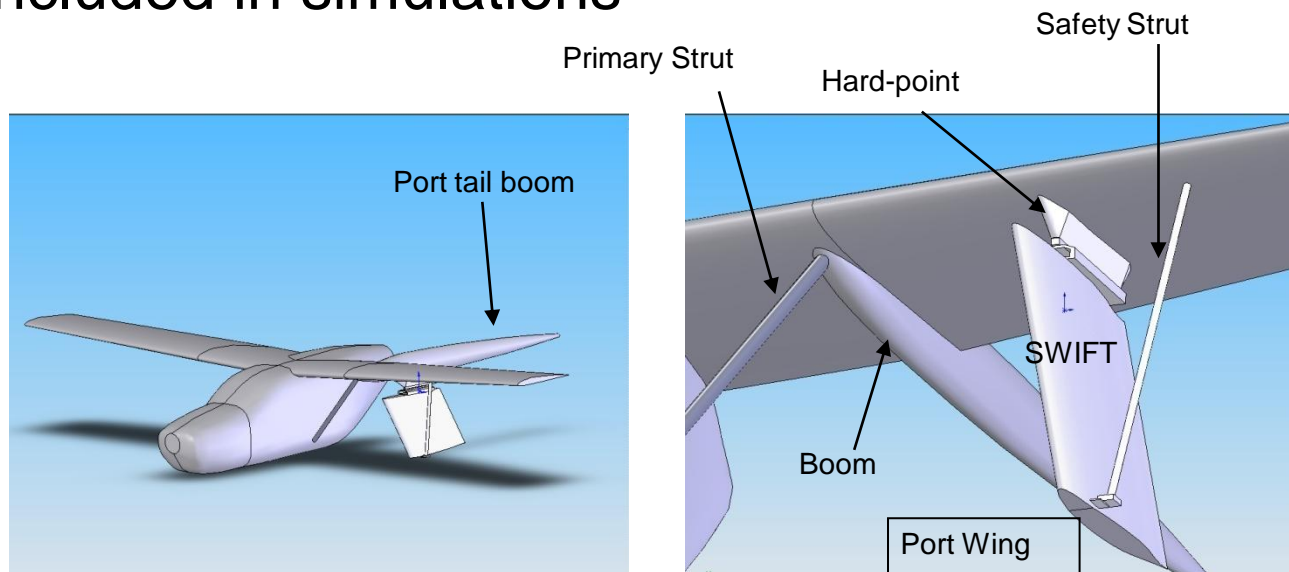
Flight Tests

- Flight tests conducted by Texas A&M Flight Research Lab
 - Aircraft: Cessna O-2A Skymaster
 - Test Article: Swept Wing In Flight Tests (SWIFT)

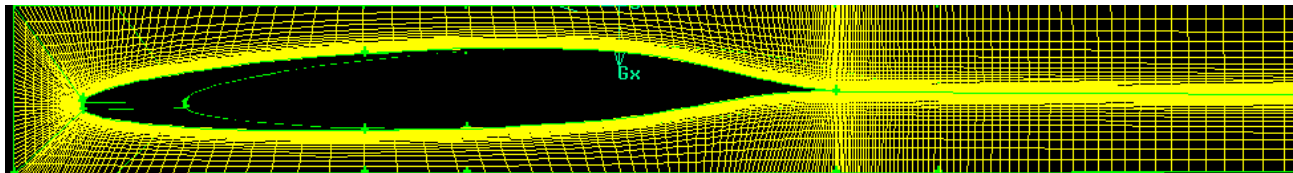
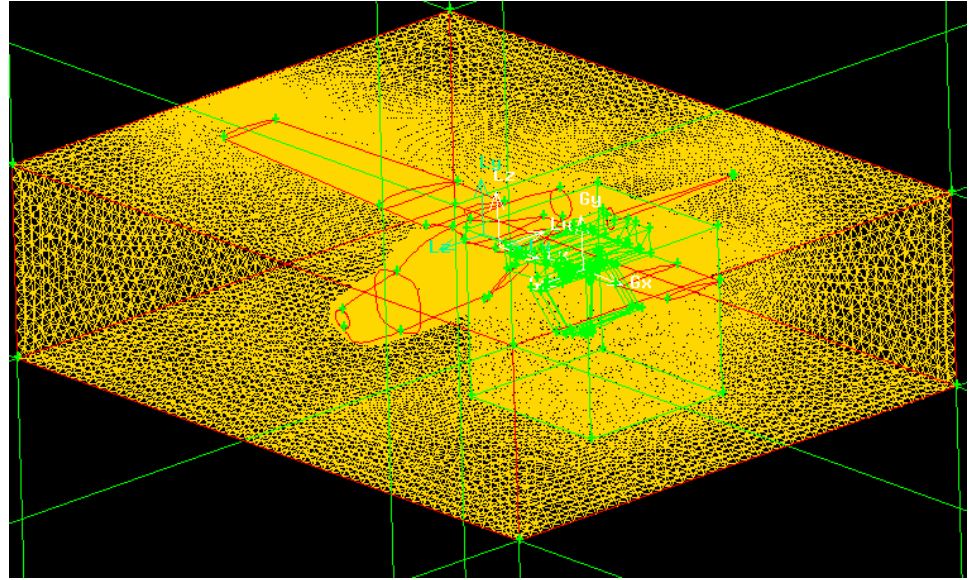
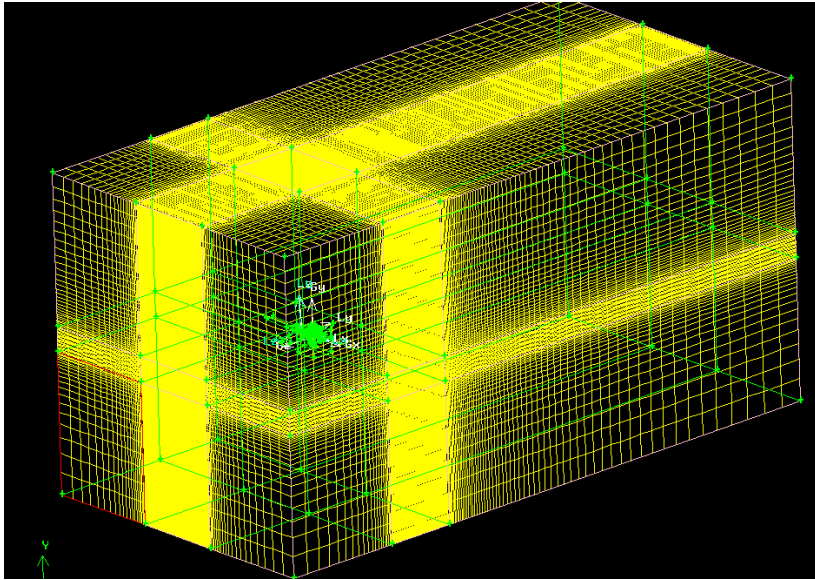


Flight Tests

- Created in Solidworks
 - Discarded horizontal and vertical tail surfaces as well as starboard tail boom, wing strut, and wing mount
 - Be sure all structures affecting model flowfield are included in simulations

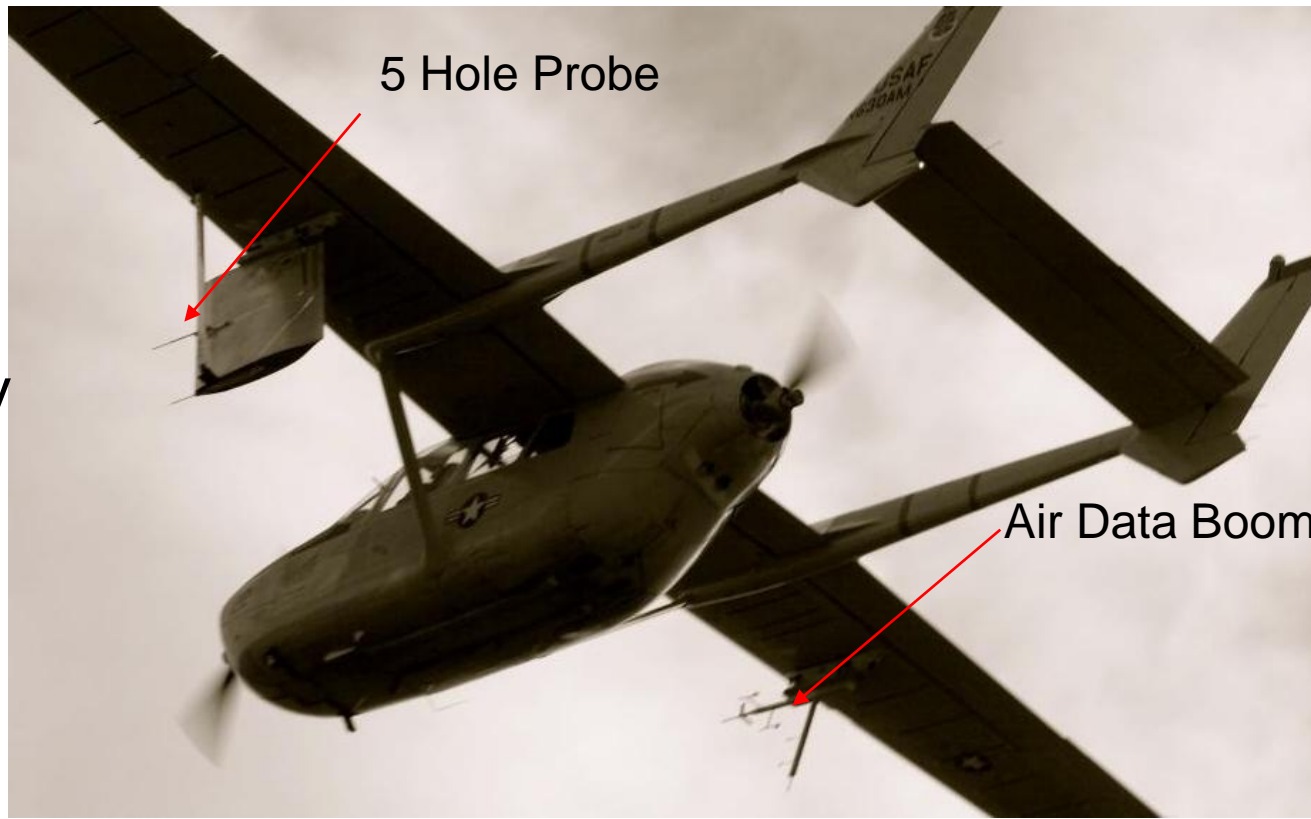


Flight Tests



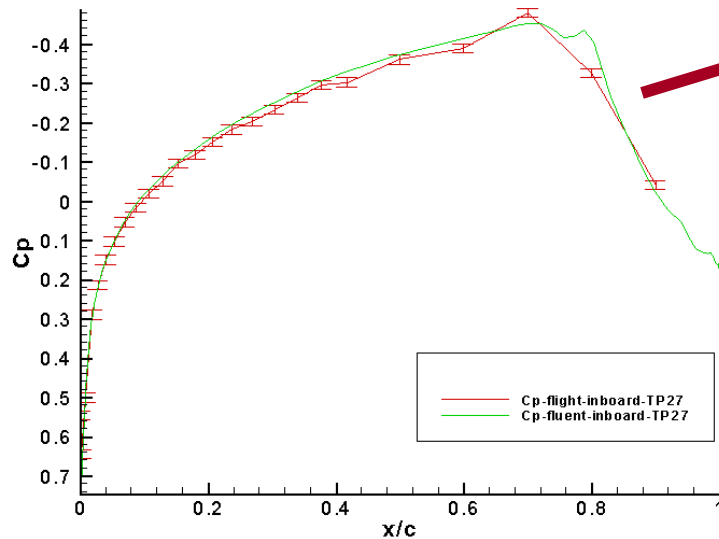
Flight Tests

- CFD aided in selecting final placement of 5-hole probe
- Iterative procedure used to back out correct up-stream condition to yield probe location angle as indicated in flight

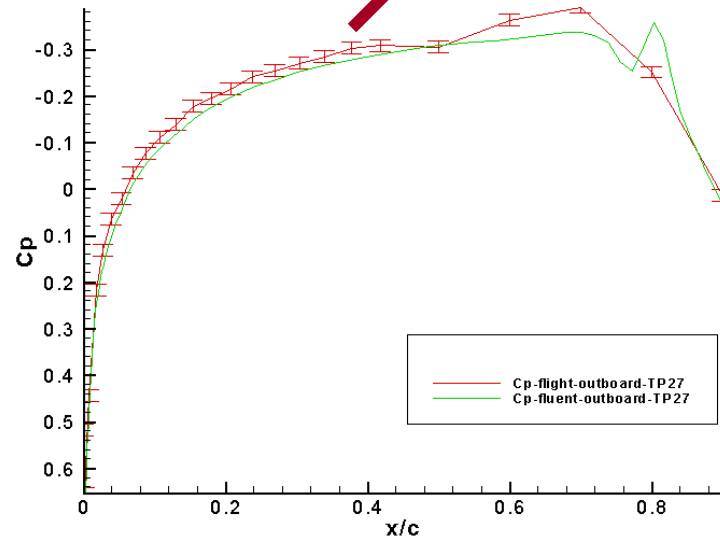


Flight Tests

- Test point 27: -4.69°
SWIFT angle of attack



Inboard C_p TP27

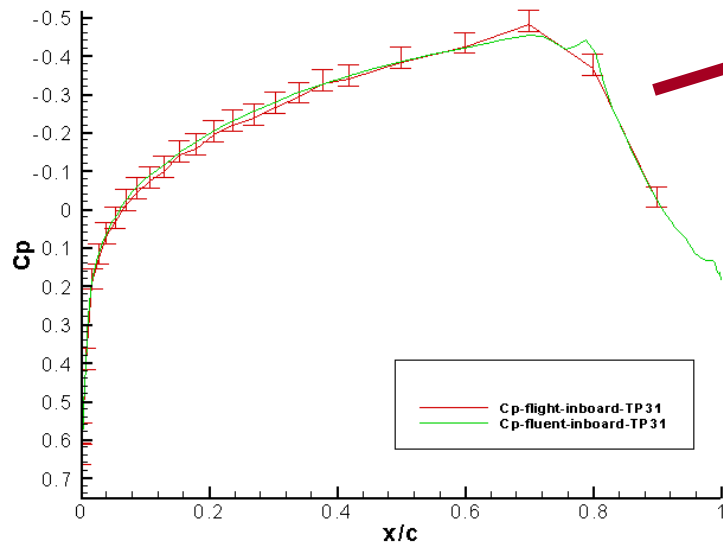


Outboard C_p TP27

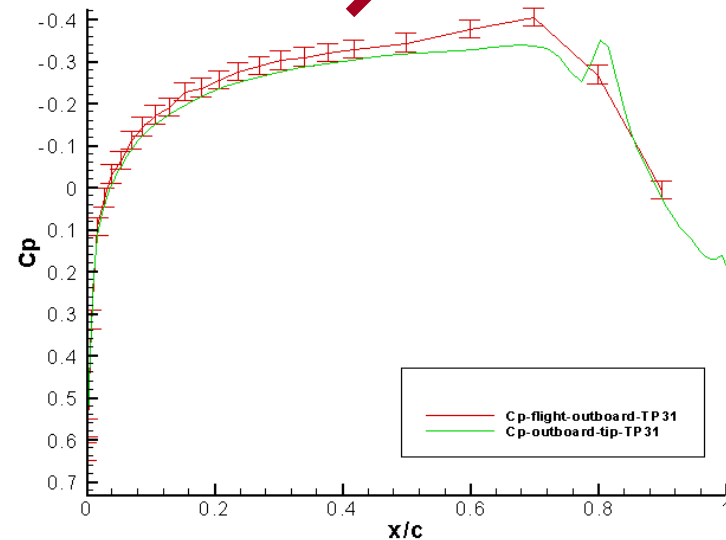


Flight Tests

- Test point 31: -2.61°
SWIFT angle of attack



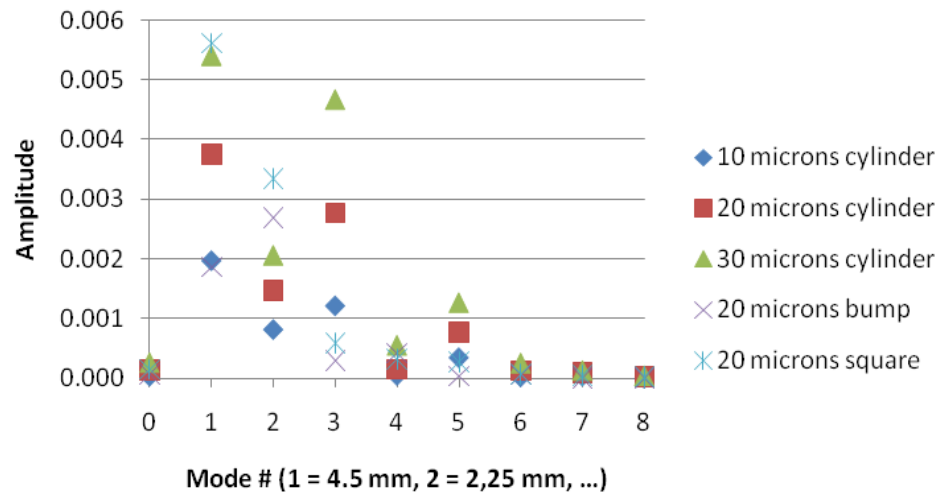
Inboard C_p TP31



Outboard C_p TP31

Crossflow - Receptivity

Roughness spectra at 2% x/c

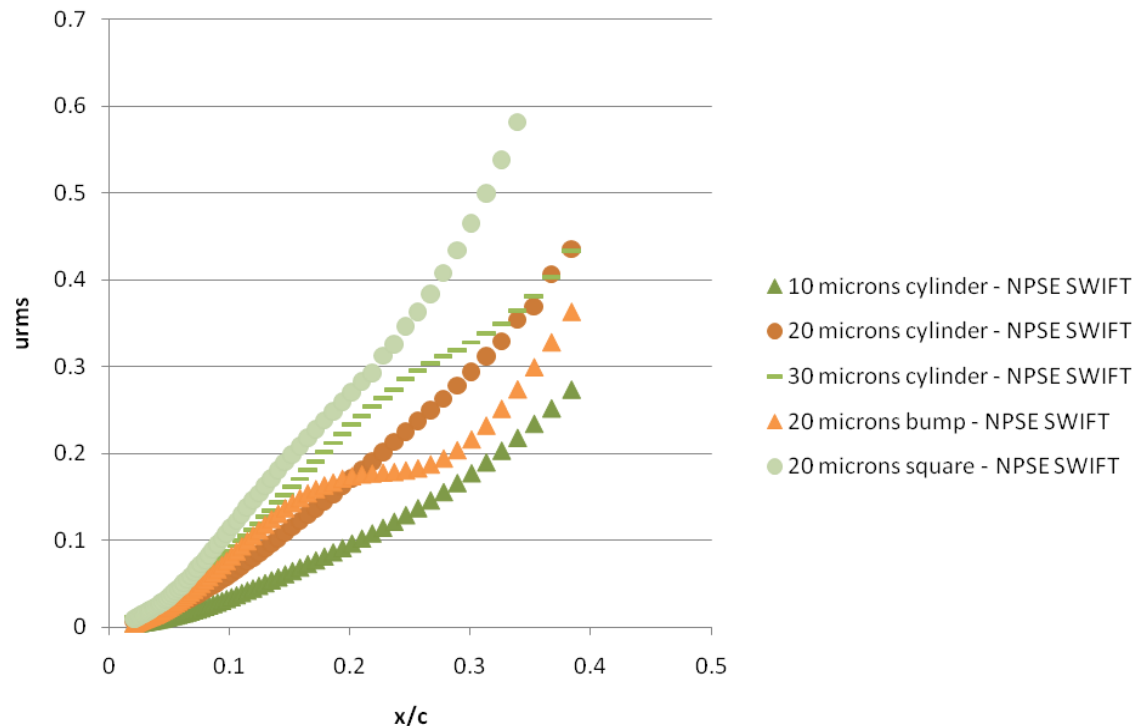


w/ Rizzetta, Visbal - AFRL

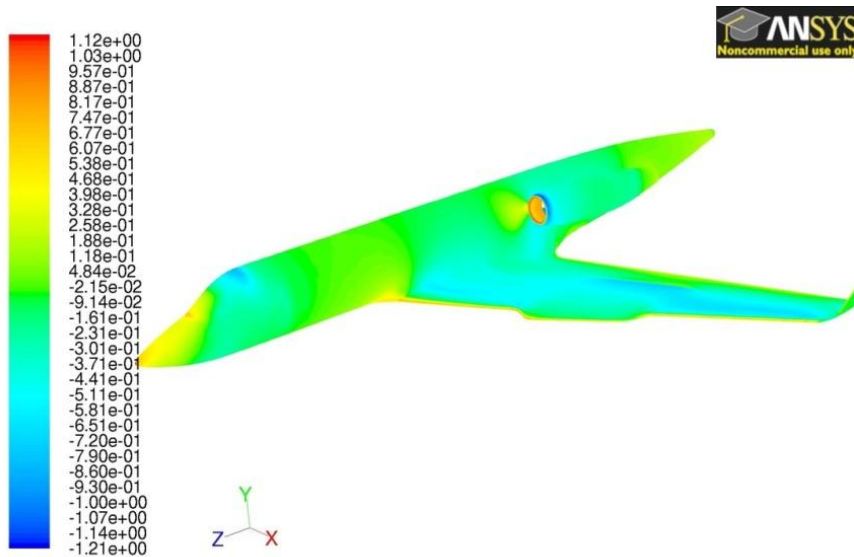
- Different roughness shapes and heights
 - Cylinders, bumps, squares
- Navier-Stokes solutions coupled with NPSE
- Roughness receptivity nonlinear and configuration dependent

Ongoing:
Companion to detailed
KSWT experiments

urms normalized with local edge speed at 2% x/c



Flight Tests



NASA Environmentally Responsible Aviation:
NASA Langley, NASA Dryden

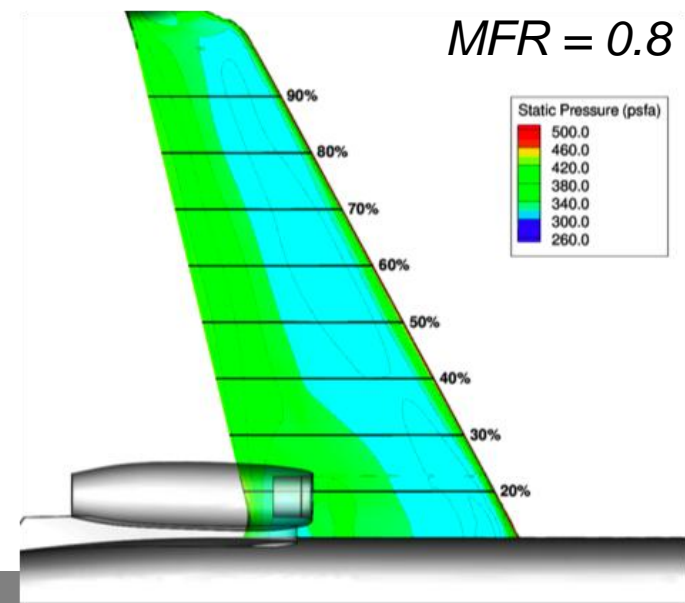
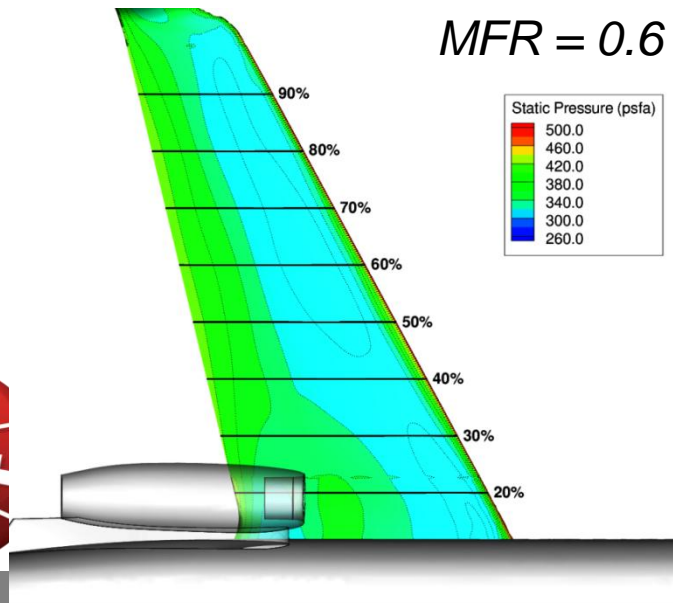
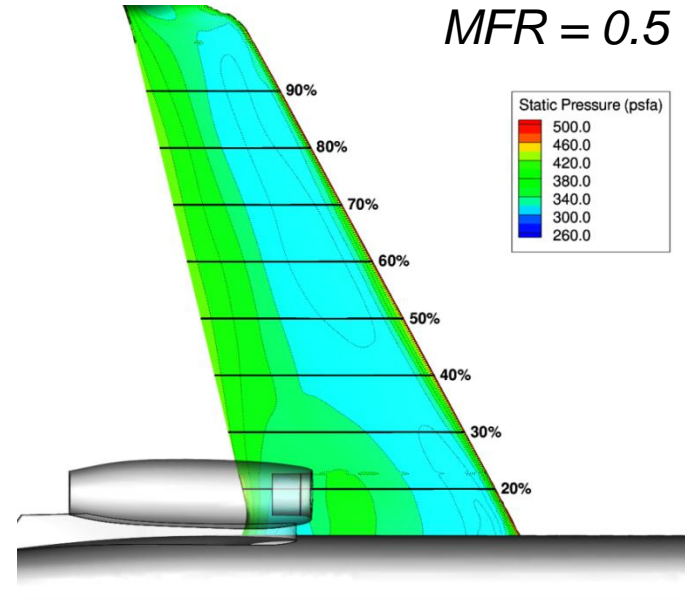
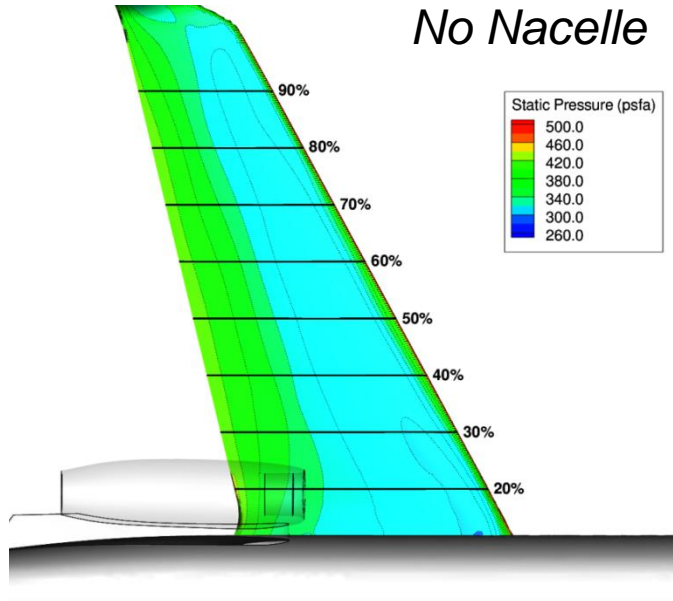
Gulfstream III

Experiment: SARGE

Demonstrate LFC 22-30M Re_c

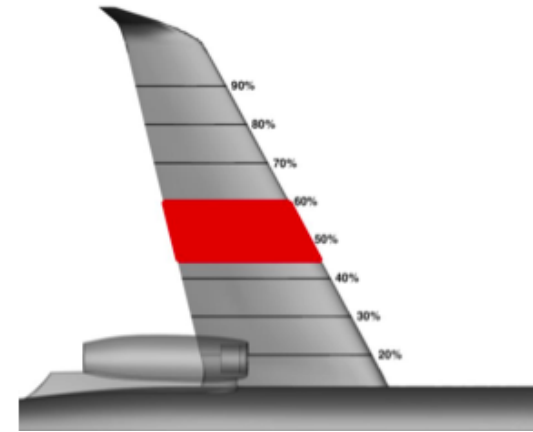


Flight Tests

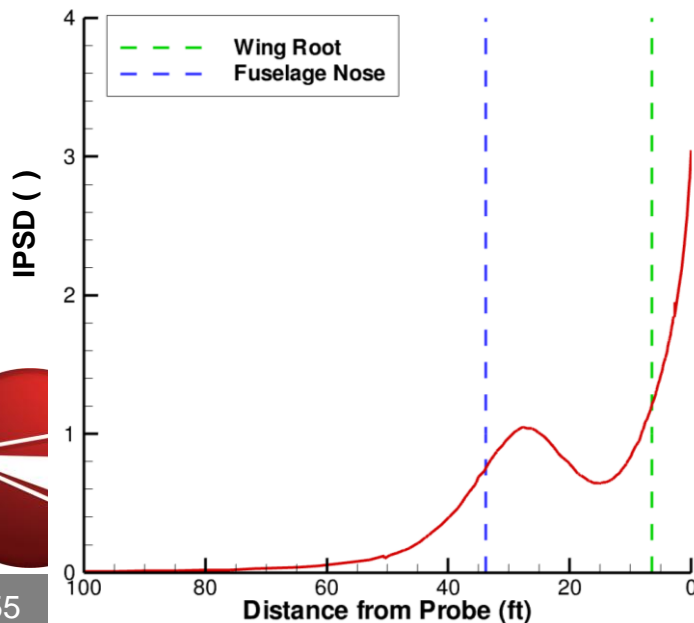


Flight Tests

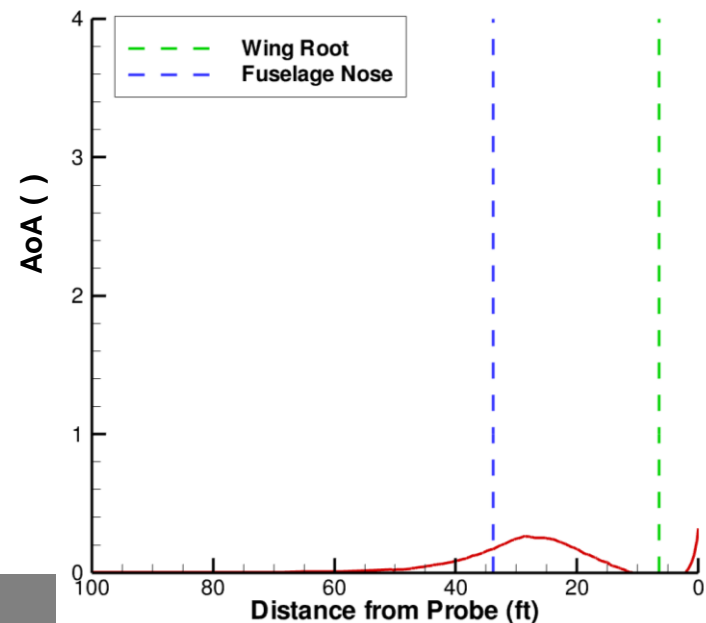
- Streamline Deflection
 - Minimal deflection in glove AoA ($\sim 0.3^\circ$)
 - Greater deflection in glove IPSD ($\sim 3^\circ$) (in-plane streamwise deflection)



Changes in wing glove IPSD

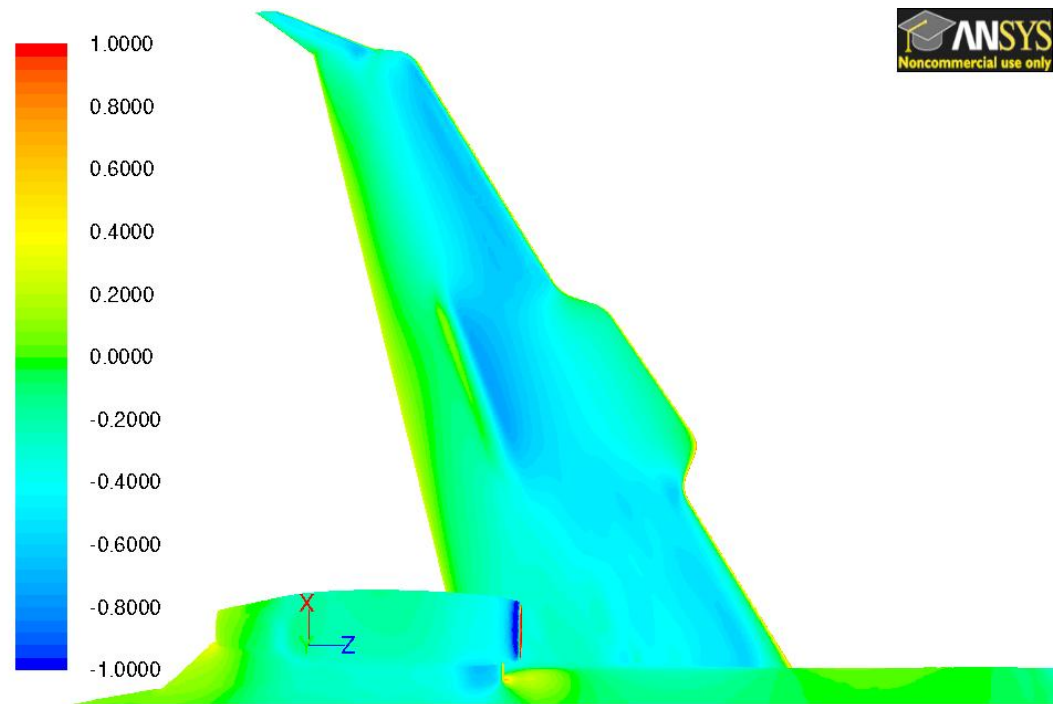


Changes in wing glove AoA



Flight Tests

- Designing G-III glove OML for LFC
 - 60% c laminar flow suction side
 - 50% c laminar flow on pressure side (*optional*)
 - Leading-edge sweep $\Lambda_{LE} = 34^\circ$, $M = 0.75$, $H \sim 40$ kft



Contours of Pressure Coefficient

Summary

- Laminar-turbulent transition highly initial- and operating-condition dependent, and finding careful, archival experiments is main validation issue; careful and well documented flight and quiet wind tunnel data are needed, especially in hypersonics (real-gas, high-enthalpy conditions).
- Routine use of our tools depends on our knowledge and modelling of initial amplitudes and disturbance mode content for upstream or inflow conditions, as well as wall conditions. Areas of boundary-layer receptivity and transient growth offer very promising breakthroughs.



Summary

- LST, NPSE, and DNS used appropriately and under appropriate physical conditions are established as viable frameworks and partners in understanding of transition mechanisms and control.
- With appropriate disturbance input conditions, agreement among theory, computations, and experiments is remarkable. Much progress over the past decades in receptivity (including roughness) and 3-D boundary layers because of groups working hand-in-hand:
 - One must perform complementary computations and experiments on same complete geometries and operating conditions.
 - Because of sensitivity of transition to initial and operating conditions, computations provide validation of experiments and vice versa.



Summary

- As we aspire to understand freestream disturbances, chemistry and thermal models, and control in high-speed, flight-Reynolds-number, and complex-geometry flows, this collaboration even more critical.
 - Detailed measurements often more difficult and costly in these flows.
 - Here, computations can guide experiments as to what effects are important and what needs to be measured.
- Experimental guidelines
 - AIAA Transition Study Group (Reshotko, Saric)
 - Saric “Wall-Bounded Flows: Boundary-Layer Stability and Transition”, Chapter 12.3, pp. 886-896, Handbook of Experimental Fluid Mechanics, eds. Tropea/Yarin/Foss, Springer, 2007
 - Berry, Kimmel, Reshotko: AIAA-2011-3415

